Nature Environment and Pollution Technology
An International Quarterly Scientific Journal

p-ISSN: 0972-6268
(Print copies up to 2016)
e-ISSN: 2395-3454

Vol. 25 | No. 2 | Article ID B4374 | 2026

Original Research Paper

https://doi.org/10.46488/NEPT.2026.v25i02.B4374

Open Access Journal

Physicochemical, Morphological and Elemental Composition Characterization of Starch Obtained from *Amorphophallus paeoniifolius* Tuber Corms

Neetu Saharan, Neeraj Wadhwa and Smriti Gaur†
Department of Biotechnology, Jaypee Institute of Information and Technology, Noida, India
†Corresponding author: Smriti Gaur; smritigaurjiit@gmail.com

Abbreviation: Nat. Env. & Poll. Technol.
Website: www.neptjournal.com

Received: 30-06-2025
Revised: 23-08-2025
Accepted: 07-09-2025

Key Words:

Amorphophallus paeoniifolius starch
Gelatinization
Plasticizers
Non-toxic biopolymer
Sustainable packaging

Citation for the Paper:

Saharan, N., Wadhwa, N. and Gaur, S., 2026. Physicochemical, morphological and elemental composition characterization of starch obtained from Amorphophallus paeoniifolius tuber corms. *Nature Environment and Pollution Technology,* 25(2), B4374. https://doi.org/10.46488/NEPT.2026.v25i02.B4374

Note: From 2025, the journal has adopted the use of Article IDs in citations instead of traditional consecutive page numbers. Each article is now given individual page ranges starting from page 1.

ABSTRACT

This study explored the potential of *Amorphophallus paeoniifolius* starch as a sustainable biopolymer for biodegradable food packaging. The isolated starch exhibited a C-type crystalline structure with 34.3% crystallinity, diverse granule morphology, and good thermal stability. Proximate composition revealed high starch content (78.61 g.100 g^{-1}) with low ash (0.17 g.100 g^{-1}) and fat (0.30 g.100 g^{-1}) content, supporting its purity and functional suitability. The presence of hydroxyl (-OH) groups further enhanced mechanical cohesion, indicating the ability to form stable biofilms. These results highlight the novelty of utilizing *A. paeoniifolius* starch as an eco-friendly, renewable, and non-toxic material with promising applications in sustainable packaging and coating technology. These properties highlight the novelty of *A. paeoniifolius* starch as a renewable, biodegradable, and functional biopolymer, supporting its application in sustainable packaging and coating technologies.

INTRODUCTION

Elephant Foot Yam (EFY), scientifically known as *Amorphophallus paeoniifolius* (*A. paeoniifolius*) and commonly referred to as "Jameenkand" in Hindi, is a tropical tuber crop extensively cultivated in humid regions across India, Southeast Asia, and Africa (Singh & Wadhwa 2014, Mukherjee et al. 2014). It belongs to the Araceae family, which comprises approximately 170 species (Mukherjee et al. 2014). EFY is renowned for its rich nutritional profile and low-fat content. In particular, it is a significant source of essential fatty acids, including Omega-3, which has been shown to positively affect cholesterol levels (Reddy et al. 2014). Additionally, EFY supports estrogen regulation in women, promoting hormonal balance, and thus holds potential as a functional ingredient to enhance human health.

Polysaccharides, such as natural gums, chitosan, alginate, carrageenan, and gellan gum, are widely used in coating development because of their functional properties. Among them, starch stands out for its biodegradability, thermoplastic nature, and aesthetic appeal, making it a preferred coating material. Starch is a semi-crystalline polysaccharide carbohydrate mainly composed of amylose and amylopectin (Sukhija et al. 2016, Kandekar et al. 2021). Amylose is a linear polymer with chains linked by α-1, 4 bonds, whereas amylopectin is a branched polymer featuring both α-1, 4 and α-1, 6 linkages (Kandekar et al. 2021, Shujun et al. 2005, Chagam et al. 2018). These structural differences are key to the wide applications of starch in the food and non-food industries (Zhang et al. 2017, Marimuthu et al. 2013). It is commonly derived from corn and potatoes and is highly valued for its ease of extraction, cost-effectiveness, and eco-friendly properties, leaving minimal environmental residue (Zhang et al. 2017, Chagam et al. 2018, Theivasanthi & Alagar 2011).

Resistant starch (RS) is a functional fiber that remains undigested in the small intestine but is partially or fully broken down in the large intestine, producing short-chain fatty acids (SCFAs) such as butyrate, propionate, and acetate. SCFAs help regulate blood glucose levels, lower the risk of colorectal cancer linked to red meat consumption, enhance postprandial lipid oxidation, and promote satiety (Geirnaert et al. 2017). RS has several advantages over traditional fibers, including a low water-holding capacity, fine particle size, and neutral flavor. As a prebiotic, RS promotes gut health and supports various physiological functions, including improved fatty acid digestion, reduced inflammation, and better glycemic control (Islam et al. 2022). Resistant starch-rich powder (RSRP), such as that from banana starch, improves bakery products by moderating starch availability and slowing carbohydrate release. Baixauli showed that replacing wheat flour with resistant starch from native maize reduced muffin volume, height, and gas cell formation (Abbas et al. 2010). It is also used in microencapsulation of probiotics in dairy products to enhance their viability, as well as in reducing oxidation and odor in fish oil (Awuchi et al. 2022). Furthermore, starch nanoparticles have gained attention for application in food packaging, plastic fillers, and medical fields for the treatment and diagnosis of cardiovascular diseases and drug delivery systems (Awuchi et al. 2022).

Starch extracted from *A. paeoniifolius* has broad applicability as a thickener, adhesive, gelling agent, stabilizer, and bulking agent. It is also used as a base material for developing edible coatings, biodegradable packaging films and active packaging films (Shujun et al. 2006). Its moderate granule size enhances its suitability for film production and food formulation (Aprianita et al. 2009). Plant-derived starches are preferred for bioplastics because they are eco-friendly, abundant, low-cost, and non-toxic, contributing to advancements in biodegradable plastic technologies (Sukhija et al. 2016, Wahyuningtiyas & Suryanto 2017). Cassava and sago starches are common in bioplastic and biofilm production, respectively, while other sources include corn, peas, oats, potatoes (sweet and white), water chestnuts, wheat, chestnuts, bananas, rye, and tapioca (Wahyuningtiyas & Suryanto 2017, Sondari et al. 2019, Özdamar & Ateş 2018). The structural composition of starch plays a key role in determining the film properties. Studies suggest that a higher amylose content can enhance the mechanical integrity of the coating and its resistance to moisture and gas transmission. According to Oyom et al., starch-based edible coatings exhibit excellent gas barrier properties owing to hydrogen bond arrangements. They are also odorless and colorless, allowing the permeation of flavoring agents into the food. However, a significant limitation is their low water resistance, which results from the intrinsic hydrophilicity of starch (Oyom et al. 2022).

Natural starch has limited industrial applications because of its weak pasting properties and undesirable gel formation upon cooling. To address this, starch is often chemically, enzymatically, and hydrolytically modified to enhance its water-holding capacity, heat resistance, binding ability, and thickening efficiency. Modified tapioca starch and lecithin improved the texture and overall quality of reduced-fat Feta cheese, whereas high-amylose cornstarch improved the texture of extruded and fried snacks (Abbas et al. 2010). Additionally, modified starches are employed in biodegradable food packaging films because of their superior physical and mechanical properties (Galvão et al. 2018).

Despite the promising attributes of *A. paeoniifolius* starch, there has been limited research on its properties. Most studies have focused on common sources such as maize and potatoes, with little exploration of the organoleptic, structural, functional, and thermal characteristics of *A. paeoniifolius* starch, which are important for industrial and food applications. Moreover, the effects of processing methods, such as alkaline extraction, on its quality are not well understood. This study aimed to fill these research gaps by isolating starch from *A. paeoniifolius* using an alkaline method and characterizing its structural, thermal, and morphological properties. Advanced analytical techniques such as Differential Scanning Calorimetry (DSC), Fourier-transform infrared spectroscopy (FTIR), X-ray Diffraction (XRD), Scanning Electron Microscopy (SEM), and energy-dispersive X-ray spectroscopy (EDX) will be employed. These analyses provide valuable insights into the physicochemical attributes of *A. paeoniifolius* starch and its potential for the development of bio-based films.

MATERIALS AND METHODS

Materials

In this study, mature corms of *A. paeoniifolius* were sourced from the local market in Modinagar, Ghaziabad, Uttar Pradesh, India. The corms were thoroughly cleaned by washing with purified water to eliminate any surface contaminants, ensuring that they were adequately prepared for subsequent experimental procedures.

Isolation of Starch

Starch was extracted from *A. paeoniifolius* following the methodologies described by Sukhija et al. (2016) and Kandekar et al. (2021). *A. paeoniifolius* corms were weighed, thoroughly washed, and then peeled. These cleaned corms were then chopped into small segments and soaked in a

solution containing 0.25% potassium metabisulfite and 0.12% citric acid for 1h. After soaking, the pieces were blended with distilled water for 5 min to form a slurry. The resulting slurry was filtered through a muslin cloth to eliminate the fibrous material from the starch suspension. The filtrate was kept at 4°C for 4 h, allowing the starch to settle at the bottom. After sedimentation, the clear supernatant was gently poured off, and the starch sediment was resuspended in water and treated with a 0.2% sodium hydroxide (NaOH) solution. The washing step was performed multiple times to ensure the removal of impurities and obtain purified starch. Finally, the starch was dried at a temperature of 45°C-50°C for 3-4 h, ground into a fine powder, and stored in an airtight container at room temperature until further analysis.

Organoleptic and Physicochemical Properties of Starch

Iodine Test, Organoleptic Properties and pH

The iodine test for starch was performed by adding two drops of iodine solution to 2 mL of a 5% starch solution, and the mixture was gently mixed and warmed in a water bath for a few minutes. The color, odor, taste, and texture of starch were carefully observed and documented. The pH of the starch samples was determined by preparing a slurry containing 1 g of starch powder in 30 mL of distilled water and measuring the pH using a calibrated pH meter at room temperature [25°C -30°C] (Yusuf et al. 2022). The starch yield percentage was determined using Equation 1 as follows:

$$\text{Starch yield (\%)} = \frac{\text{Weight of extracted starch}}{\text{Weight of } A.\ paeoniifolius} \times 100 \quad \ldots(1)$$

Proximate/Chemical Composition Analysis of Starch

The proximate and chemical compositions of *A. paeoniifolius* starch were analyzed in accordance with standardized protocols of the International Organization for Standardization (ISO) and Food Safety and Standards Authority of India (FSSAI) certified laboratory (Advanced Research & Analytical Services, Ghaziabad, Uttar Pradesh, India). Moisture, ash, and starch contents were determined according to (IS 4706-2) (Bureau of Indian Standards (BIS) 1978), while protein content was quantified using the Kjeldahl method (IS 7219-1973), with a conversion factor of 6.25 applied to calculate the protein content. Fat content was estimated using the Soxhlet extraction method (IS 4684-1975), and sugar content was measured according to IS 2650-1975. The carbohydrate content was determined following IS 1656-2022, and the energy content was computed from the proximate composition as per IS 9487-1981. Dietary fiber was quantified gravimetrically using the methodology outlined in IS 11062-2019.

Fourier Transform Infrared Spectroscopy (FTIR)

The functional characterization of *A. paeoniifolius* starch granules was performed using FTIR spectroscopy on a Shimadzu FTIR Spectrophotometer (Japan) at the Department of Material Characterization Laboratory, Jaypee Institute of Information Technology, Noida. A finely powdered starch sample was thoroughly combined with spectroscopic-grade potassium bromide (KBr) in a 1:100 proportion to obtain a homogeneous mixture for FTIR analysis. KBr, being spectroscopically inert, was selected to facilitate the formation of translucent pellets that allow effective transmission of infrared light. The combination was then compressed into a translucent pellet using a hydraulic press under high pressure. Spectral data were recorded in the wavenumber range of 4000–400 cm^{-1} to enable the precise identification of functional groups and molecular interactions (Marichelvam et al. 2019).

Thermal Analysis Using Differential Scanning Calorimetry (DSC)

The thermal behavior of starch was analyzed using DSC. For this analysis, a 5 mg starch sample was accurately weighed and placed in a DSC sample pan. The analysis of the starch granules was carried out using a HITACHI DSC 7000 system, operated with a computerized analyzer at the Department of Material Characterization Laboratory, Jaypee Institute of Information Technology, Noida. The scanning was conducted under a nitrogen atmosphere, applying a constant heating rate of 10°C per minute, across a temperature range of 30°C to 160°C (Kandekar et al. 2021, Esquivel-Fajardo et al. 2022).

Morphological Characterization of Starch by Scanning Electron Microscopy (SEM)

The surface morphology of *A. paeoniifolius* starch granules was examined using SEM with a ZEISS EVO40 microscope at Jawaharlal Nehru University, New Delhi. For SEM preparation, isolated starch samples were gently dusted onto double-sided adhesive carbon tape, which was mounted on aluminum stubs to ensure stable adhesion of the samples. The samples were then sputter-coated with a thin layer of gold to enhance their conductivity. Imaging was conducted at an accelerating voltage of 20 kV to enable detailed visualization of the starch granule structures. This methodological approach facilitates high-resolution imaging, revealing critical insights into granule morphology and surface characteristics (Sukhija et al. 2016, Wahyuningtiyas & Suryanto 2017).

Energy Dispersive X-Ray Spectroscopy (EDX)

In this analysis, a starch sample was subjected to X-ray

bombardment, causing the emission of characteristic X-rays specific to each element. The emitted X-rays were subsequently detected and analyzed using an EDX detector at Jawaharlal Nehru University, New Delhi. The resulting spectrum provided a detailed compositional profile, identifying key elements within the alloy, such as carbon (C), oxygen (O), and hydrogen (H), as indicated by spectral peaks in accordance with referenced studies (Sukhija et al. 2016, Wahyuningtiyas & Suryanto 2017).

X-Ray Diffraction (XRD)

XRD analysis of the starch sample was conducted at the Department of Material Characterization Laboratory, Jaypee Institute of Information Technology, Noida. The analysis was performed using an X-ray diffractometer equipped with a Cu-Kα radiation source (wavelength = 1.54056 Å). The device was operated at a voltage of 40 kV and a current of 30 mA. The scanning procedure covered a 2θ range 10° to 80° to investigate the structure of starch. Data were collected in continuous scan mode at a scanning speed of 2.0° per minute, and a 15 mm receiving slit was used to ensure high-resolution diffraction patterns. This setup provided a detailed examination of the crystallographic properties of the starch sample (Theivasanthi & Alagar 2011).

RESULTS AND DISCUSSION

Assessing Starch Yield and Its Physicochemical and Organoleptic Properties

The percentage yield of starch extracted from *A. paeoniifolius* was 1.2%, with 6 g of starch recovered from 500 g of fresh tubers. These results revealed variations in starch content among different tuber sources, highlighting the significant influence of tuber type on starch extraction efficiency. The starch obtained from *A. paeoniifolius* tested positive for the iodine test, exhibited a white color, had a fine texture, was odorless, tasteless, and was insoluble in both water and alcohol, and had a pH of 6.10. Similar findings were reported by Yusuf et al. (2022), who also obtained positive results for the iodine test on native and silicified starch samples obtained from Ipomoea batatas. The color of their samples was white, and both native and silicified samples were noted to be odorless, tasteless, and had a fine texture. A study by Jubril et al. (2012) reported that phosphate starch, pregelatinized starch, and sweet potato starch powders turned blue-black upon the addition of iodine solution, further confirming the presence of starch.

Proximate and Chemical Composition Analysis

Proximate composition is a reliable method for assessing starch purity, where more starch and less protein, fat, ash, and fiber are preferred. Excess protein and fat can affect swelling and pasting properties by interacting with starch granules and reducing gelatinization (Schoch 1968, Olkku & Rha 1978, Liang & King 2003, Lumdubwong & Seib 2000). A previous study showed that proteins can change the gelatinization and pasting behavior of starch, highlighting their significant role in functionality (Hamaker & Griffin 1993). Therefore, proximate and chemical analyses are essential for evaluating the fundamental composition of food and agricultural products. The results for the starch isolated from *A. paeoniifolius* are summarized in Table 1.

Table 1: Proximate/chemical analysis of *Amorphophallus paeoniifolius* starch.

Test Parameters	Value [g.100g^{-1}]	Test Method
Moisture	11.8	IS:4706
Total Ash	0.17	IS:4706
Starch	78.61	IS:4706
Protein	6.76	IS:7219
Total fat	0.30	IS:4684
Total sugar	BDL(DL-0.5)	IS:2650
Carbohydrate	81.19	IS:1656
Dietary Fiber	2.58	IS: 11062
Energy	354.50 Kcal.100g^{-1}	IS:9487

Analysis of Moisture Content

Moisture content is critical in determining the texture, stability, and application performance of starch. Excess moisture can cause clumping, whereas insufficient moisture can lead to brittleness. In this study, *A. paeoniifolius* starch showed a moisture content of 11.8%, which falls within the range reported for purple-fleshed sweet potatoes (PFSP) (8.52% and 14.86%) (Julianti et al. 2018). Variability in starch moisture depends on factors such as drying conditions and seed structure (Andrabi et al. 2016,Kaur & Sandhu 2010). Lower moisture content enhances storage stability by reducing microbial activity (Alozie et al. 2009). The relatively low moisture content observed here suggests a better shelf life and reduced risk of microbial contamination.

Analysis of Ash Content

The ash content indicates the total mineral residue after the combustion of organic matter. In this study, the ash content of A. paeoniifolius starch was 0.17%, which is low and comparable to that of purple-fleshed sweet potato (PFSP starch, 0.26% and 0.36%; Julianti et al. 2018). Such a low ash value suggests minimal mineral impurities, which is desirable for applications requiring high-purity starches.

Analysis of Fat Content

Fats play an important role in food systems by providing

energy, enhancing flavor, and influencing the storage stability of flour-based products (Titov 2012, Levitsky et al. 2020, Boahemaa et al. 2024). The fat content of *A. paeoniifolius* starch was 0.30%, as determined by the Soxhlet technique. This value is lower than that of PFSP starch (Julianti et al. 2018).) reflecting minimal lipid presence. Such low-fat content is advantageous for storage stability and for applications requiring starch with reduced lipids.

Analysis of Dietary Fiber

Dietary fiber (DF) refers to non-digestible plant components that are partially or fully fermented in the large intestine of the host. It plays an important role in functional foods and contributes to health benefits, such as lowering blood sugar and lipid levels and reducing the risk of gastrointestinal disorders (He et al. 2022, Boahemaa et al. 2024). In this study, *A. paeoniifolius* starch showed a dietary fiber content of 2.58%, which falls within the range reported for purple-fleshed sweet potatoes (0.25–2.59%, Julianti et al. 2018). The low DF content confirms its predominance as a carbohydrate source, with minimal fiber residue.

Analysis of Carbohydrate and Energy

Carbohydrates are the major source of dietary energy and structural components in living organisms (Cummings & Stephen 2007, Witek et al. 2022). In this study, *A. paeoniifolius* starch contained 81.19% carbohydrates, similar to taro (77.82–86.11%) and yam (75.98–84.07%) (Ijarotimi et al. 2015, Kibret Akalu & Haile Geleta 2019), but higher than that of sweet potato (20.28–35.12%) (Omodamiro et al. 2013). The calculated energy value (354.50 Kcal.100 g^{-1}) was also comparable to that of other root starches, supporting its role as an energy-dense food source. The sugar content was below the detection limit (<0.5 g), consistent with Meludu (2010).

Analysis of Starch Content

Starch is the major storage polysaccharide in plants and is a key dietary carbohydrate (Omar et al. 2016). In *A. paeoniifolius* corms, starch content was 78.61%, higher than PFSP (50.20–62.93%) (Julianti et al. 2018) but within the range reported for other tubers (92–96%) (Abegunde 2012). The overall composition—high starch (78.61%), low ash (0.17%), low fat (0.30%), and moderate fiber (2.58%)—suggests its suitability for biofilm formation, where starch provides structural integrity, and reduced mineral and lipid contents enhance mechanical and barrier properties.

Analysis of Protein Content

Proteins are essential nutrients that not only support human health but also influence functional properties, such as water and oil absorption, gelation, and rheology, which are critical in food product development (Boahemaa et al. 2024). Plant-derived proteins, such as those from soy, rice, and wheat, have been shown to promote gut health and microbial balance (Ashaolu 2020, Huang et al. 2016).

In this study, the protein content of *A. paeoniifolius* was found to be 6.76%, as determined using the Kjeldahl method. The presence of moderate protein content in *Amorphophallus* starch may enhance certain functional properties, such as mechanical strength, tensile strength, and flexibility, in biofilm applications. These findings suggest that *A. paeoniifolius* starch is a promising candidate for sustainable and biodegradable food packaging. These findings align with research by Julianti and coworkers (Julianti et al. 2018), which highlights the potential of *Amorphophallus* starch for developing eco-friendly biofilms with desirable mechanical and barrier characteristics, essential for sustainable packaging applications.

Fourier Transform Infrared Spectroscopy (FTIR) Spectral Analysis

FTIR spectroscopy was used to identify the functional groups in the starch isolated from *A. paeoniifolius* by analyzing the peak values within the infrared region. This analysis provides insights into the structural characteristics of starch. The obtained data are graphically represented in Fig. 1, which displays the FTIR spectrum of *A. paeoniifolius*, illustrating transmittance (%) as a function of wavenumber (cm^{-1}). A broad absorption band observed at approximately 3000 cm^{-1} is attributed to O-H stretching vibrations, indicative of hydroxyl (–OH) groups, suggesting the presence of hydrogen bonding typically associated with starch and other polysaccharide compounds (Araújo et al. 2020, Abdullah et al. 2018). The peak at 2390 cm^{-1}, although rare in starch, may correspond to C≡C or C≡N triple bond stretching, potentially indicating trace impurities or unique molecular interactions within the sample. A weak absorption band near 1870 cm^{-1} may be related to higher vibrations or minor C=O stretching, although such features are uncommon in the standard starch profile (Araújo et al. 2020, Abdullah et al. 2018). Peaks at 1600 cm^{-1} and 1527 cm^{-1} are often associated with C=O stretching or N-H bending vibrations, characteristic of amide groups, which may indicate minimal protein residues retained from the starch extraction process. The bands around 1455 cm^{-1} and 1398 cm^{-1} likely correspond to C-H bending or scissoring vibrations, specifically linked to CH_2 groups. The absorption peak at 1270 cm^{-1} is attributed to C-O stretching vibrations, which are commonly observed in polysaccharides and are indicative of glycosidic linkages within the starch structure. Additionally, the peaks at 946

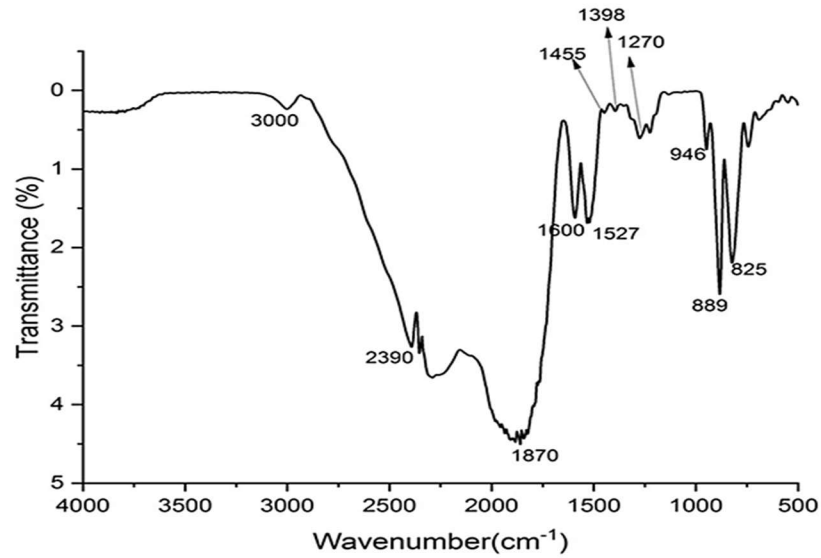

Fig. 1: FTIR spectra of *Amorphophallus paeoniifolius* starch, showing characteristic absorption bands corresponding to functional groups.

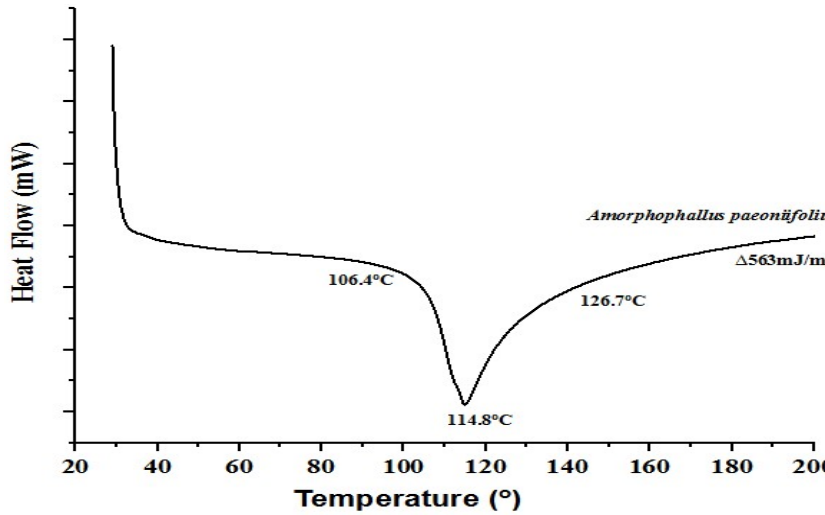

Fig. 2: Differential scanning calorimetry (DSC) curve of *Amorphophallus paeoniifolius* starch showing thermal transitions during gelatinization.

cm^{-1} and 889 cm^{-1} are consistent with C-O-C stretching, which is characteristic of glycosidic bonds and supports the polysaccharide framework typical of starch (Araújo et al. 2020, Abdullah et al. 2018). A band at 825 cm^{-1} may be associated with C-H out-of-plane bending, which is often representative of the polysaccharide backbone structure. The observed spectral features align with the findings of Julianti et al. (2018), Araújo et al. (2020), and Abdullah et al. (2018), who reported similar absorption patterns in starch samples. This alignment supports the structural integrity and purity of *A. paeoniifolius* starch, reinforcing its suitability for further applications in food and biopolymers.

Thermal Analysis of Starch Using Differential Scanning Calorimetry (DSC)

Gelatinization is a process in which starch undergoes structural breakdown upon exposure to heat and moisture. This transformation begins with the hydration and swelling of the amorphous regions within the starch granules, which induces stress on the crystalline regions, ultimately leading to their rupture and the melting of the granules. The peak temperature (Tp) at which this transition occurs is influenced by the structural arrangement and molecular composition of amylose and amylopectin in the starch matrix (Gupta & Gaur 2024). The enthalpy change (ΔH), measured by

DSC, quantifies the heat absorbed during all endothermic events that occur during the heating process. Several factors, including moisture content, solvent type, degree of hydration, botanical origin, and physical granule properties, influence ΔH values (Alonso-Gomez et al. 2016). Studies have shown that lower moisture content correlates with higher gelatinization temperatures, which is a significant factor in low-moisture systems such as baked goods or starch-based biofilm plasticization (Zuo et al. 2019).

The DSC thermogram of *A. paeonifolius* starch, shown in Fig. 2, provides valuable insights into its thermal properties, including enthalpy change and melting temperature. The thermogram reveals an onset temperature of 106.4°C, where the thermal transition initiates, followed by the peak of the endothermic process at 114.8°C, and concluding at 126.7°C. The enthalpy change (ΔH) was measured as 563 $J.g^{-1}$. These results align with the thermal characteristics typically observed for starches and are consistent with the findings reported by Kandekar et al. (2021). Among various starches, potato starch has the lowest gelatinization temperature, approximately 62°C, whereas corn and cassava starches exhibit higher gelatinization temperatures, at approximately 66°C and 68°C, respectively (Gernat et al. 1990, Lumdubwong & Seib 2000). Higher crystallinity generally contributes to greater thermal stability, which in turn raises the gelatinization temperature. This effect was further influenced by the amylopectin chain length. Precise control of the gelatinization temperature is crucial for bioplastic production. Temperatures below 60°C can result in premature gelatinization during drying, whereas excessively high temperatures increase energy costs (Abdullah et al. 2018).

Morphological Characterization of Starch Obtained from *A. Paeoniifolius* by Scanning Electron Microscopy (SEM)

The SEM is a highly versatile instrument that is widely used to examine the microstructural morphology and characterize the chemical composition of various materials (Zhou et al. 2007). SEM operates based on electron emission, providing high-resolution gray scale images that offer detailed insights into the surface structure of a sample. Fig. 3A, 3B, and 3C present scanning electron microscopy (SEM) micrographs of *A. paeoniifolius* starch granules at different magnifications (2.50 KX, 1.20 KX, and 3.25 KX, respectively), illustrating variations in morphology, size, and surface characteristics. Fig. 3A (2.50 KX magnification) offers a close-up of individual starch granules, revealing the morphological heterogeneity of *A. paeoniifolius* starch, with irregular, polygonal, and rounded granules of variable sizes, predominantly smooth surfaces, and occasional indentations. The variability in granule size observed in this study is typical of starches from diverse plant sources. Fig. 3B (1.20 KX magnification) provides a broader view of the granule distribution, displaying a clustering tendency that suggests intergranular interactions. Such aggregation can potentially influence properties such as water absorption and gelatinization, which are critical for certain applications. Fig. 3C (3.25 KX magnification) allows for a detailed examination of the granule surfaces, showcasing minor irregularities and reinforcing the diversity in shape and size, with granules ranging within the micrometer scale range. The tight packing of granules suggests a natural tendency for aggregation, which may impact their functional properties in food and biopolymer applications. Similar morphological diversity has been noted in previous studies, linking granule characteristics to plant origin (Sukhija et al. 2016). Granule size, shape, and clustering behavior significantly influence physicochemical properties, such as swelling power, light transmittance, water-binding capacity, and amylose content, which are essential for functional applications (Cone & Wolters 1990).

Energy Dispersive X-ray Spectroscopy

Energy Dispersive X-ray Spectroscopy (EDX), used

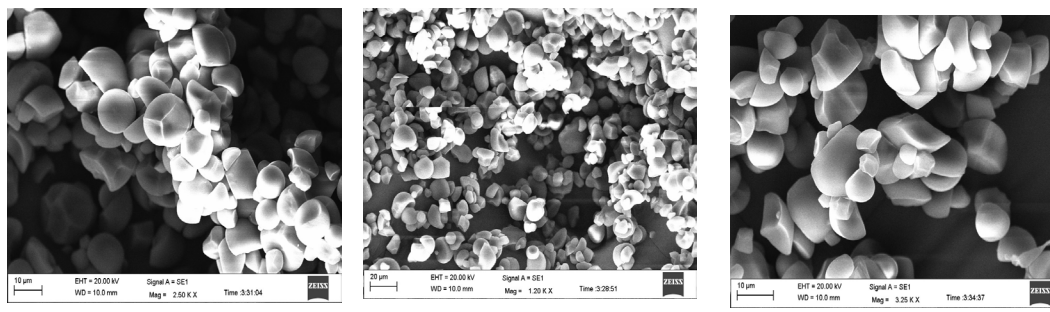

Fig. 3: SEM images of *Amorphophallus paeoniifolius* starch at different magnifications: (A) 2.50 K, (B) 1.20 K, and (C) 3.25 K, depicting the morphology of starch granules.

alongside SEM, is a powerful analytical technique for obtaining qualitative and semi-quantitative data on a sample's elemental composition (Mohammed & Abdullah 2018). EDX enables the identification of elements within a specimen using advanced computer software, offering insights that are not accessible via conventional tests. Fig. 4 shows the EDX analysis of *A. paeoniifolius* starch, revealing prominent peaks of carbon (C) and oxygen (O), which are characteristic of carbohydrate-rich compounds. Based on the quantitative data, the weight percentages (wt. %) of carbon and oxygen in starch are36.75% and 63.25%, respectively. These values were further confirmed by the normalized weight percentages. The atomic percentages revealed that oxygen had a slightly higher concentration (56.37%) than carbon (43.63 %). The error margins associated with each element suggest a reasonable degree of accuracy in these measurements, although a higher error margin of 22.3% was noted for carbon. Similar compositional results have been reported by Sukhija et al. (2016) and Wahyuningtiyas and Suryanto (2017), demonstrating the consistency of these findings.

The SEM image in the spectrum displays the granular morphology of the starch at a high magnification. This morphological observation allows for a correlation between the structural characteristics and elemental composition derived from the EDX analysis, providing a more comprehensive understanding of the physicochemical properties of starch. Such insights are crucial for evaluating the material's suitability for applications in biodegradable film production and food packaging, where both the composition and structure play significant roles. It is important to note that EDX analysis primarily detects elements with atomic numbers above approximately 4–5. This limitation arises from the fundamental mechanism of EDX, which relies on the detection of characteristic X-rays emitted when atoms are excited by an electron beam. Owing to its low atomic number and lack of high-energy X-ray emissions, hydrogen (atomic number 1) remains undetectable in standard EDX. Consequently, only heavier elements, such as carbon and oxygen in *A. paeoniifolius* starch, were observable in the spectrum.

X-ray Structural Characterization

Within the starch structure, amylopectin chains adopt a helical conformation due to the coiling of glucose monomers. These helices intertwine to form double helices, which are systematically arranged, contributing to the crystalline nature of starch. Amylose and branched regions of amylopectin play crucial roles in supporting this structural organization, primarily by forming the amorphous regions of starch (Gupta & Gaur 2024). The nanoscale structure of *A. paeoniifolius* starch was analyzed using X-ray Diffraction (XRD), as illustrated in Fig. 5. Indexing, a crucial step in structural characterization, was used to determine the unit

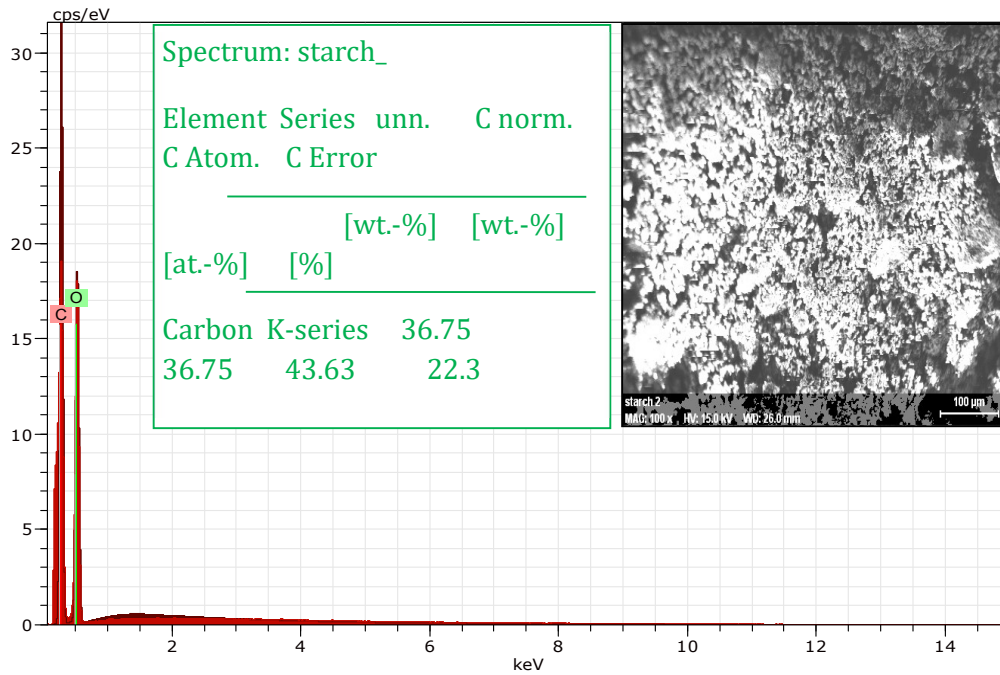

Fig. 4: EDX analysis of the *A.paeoniifolius* starch.

Table 2: Miller indices, Bragg angles, and interplanar spacing of *Amorphophallus*. *paeoniifolius* starch.

Miller indices [hkl]	2θ of peak [deg]	d-spacing [Å]
112	14.80	5.9823
020	15.17	5.8373
013	16.80	5.2744
103	17.16	5.1645
121	17.90	4.9527
022	18.20	4.8717
123	22.92	3.8780
213	23.70	3.7521

cell dimensions and arrangement based on the diffraction peaks. This process involved assigning Miller indices (h k l) to specific peaks, providing insights into the crystal structure of the starch. In this study, the primary peak reflections identified were 112, 020, 013, 103, 121, 022, 123, and 213, as listed in Table 2. These reflections reveal the key structural aspects of starch at the nanoscale. The broad peaks in the XRD profile indicate a small crystallite size, a typical feature of nanocrystalline materials, which influences properties relevant to biodegradable films and biopolymer applications.

The size of the starch particles was calculated using the Debye-Scherrer formula, as referenced in the studies by Marimuthu et al. (2013) and Theivasanthi & Alagar (2011). Particle size and distribution are critical characteristics of particle systems, as they influence the in vivo distribution, biological behavior, toxicity, and targeting efficiency of the particles. Research has consistently demonstrated that particles in the sub-micron range offer significant advantages over microparticles, particularly as drug delivery systems, owing to their enhanced bioavailability and targeted delivery potential (Marimuthu et al. 2013, Theivasanthi &Alagar 2011). The average particle size, the Debye-Scherrer equation (Equation 2) was applied to determine the average particle size, which is commonly used to estimate crystallite sizes based on the broadening of X-ray diffraction peaks.

$$D = \frac{K\lambda}{\beta Cos\theta} \quad \ldots(2)$$

Here, 'D' is the average particle size, 'K' is the shape factor (typically around 0.9 for spherical particles), 'λ' is the X-ray wavelength (usually 0.1541 nm), 'β' is the full width at half maximum (FWHM) of the diffraction peak (in radians), and 'θ' is the Bragg angle. The calculated particle size data are presented in Table 3. Additionally, the interplanar spacing, which represents the distance between atomic planes, was calculated using Bragg's Law (Equation 3). This approach offers a comprehensive understanding of the structural characteristics of *A. paeoniifolius* starch particles, allowing for a more precise evaluation of their potential applications in fields such as biomedicine and material science.

$$2d\sin\theta = n\lambda \quad \ldots(3)$$

XRD-Starch Analysis and Quantification of Crystallinity

XRD analysis of the sample revealed a B-type diffraction pattern, which is characteristic of crystalline starch structures commonly observed in tuber starches. Intermediate-intensity peaks at 2θ angles of 17.52° and 18.22° aligned with this pattern, consistent with the findings of Zobel (1988). Additionally, a prominent peak appeared at 2θ = 23.12°, and a less pronounced hump at 15.01° resembled an A-type diffraction pattern, typically associated with cereal starches. Interestingly, EFY starch displayed a C-type diffraction pattern, a hybrid of A and B types, which contrasts with the results reported by Reddy et al. (2014). Both A- and B-type starches exhibit identical double helices but differ in their packing arrangements and moisture content. The A-type crystalline structure is characterized by densely packed helices, which typically accommodate four water molecules. In contrast, the B-type structure adopts a more open hexagonal arrangement, incorporating up to 36 water molecules in the unit cell. These diffraction patterns are

Table 3: Grain size of *Amorphophallus paeoniifolius* starch from XRD.

2θ of peak [deg]	Miller indices [hkl]	FWHM (Full Width at Half Maximum) peak [β] [radians]	Size of particle [D] nm	d- spacing [nm]	d- spacing [Å]
14.80	112	0.0145	9.9043	0.5982	5.9823
15.17	020	0.0099	14.4470	0.5837	5.8373
16.80	013	0.0140	10.3777	0.5274	5.2744
17.16	103	0.0131	11.0908	0.5165	5.1645
17.90	121	0.0129	11.2867	0.4953	0.49527
18.20	022	0.0171	8.5371	0.4872	4.8717
22.92	123	0.0187	8.0646	0.3878	3.8780
23.70	213	0.0201	7.5577	0.3752	3.7521

influenced by factors such as amylopectin chain length, amylose content, and the biological source of starch (Saikia & Konwar 2012). From a crystallographic perspective, starch has been observed to exhibit two primary crystal structures: orthorhombic and hexagonal. Rodriguez-García et al. 2021 reported that starches with an orthorhombic arrangement are classified as A-type, while those with a hexagonal structure are labeled as B-type. Starches exhibiting a combination of these structures are classified as C-type (Esquivel-Fajardo et al. 2022). The XRD pattern of *A. paeoniifolius* starch in this study indicates the presence of both hexagonal and orthorhombic crystal structures, thereby categorizing it as C-type, as depicted in Fig. 5. The pattern of coexistence of both structural types within the crystalline regions aligns with the findings reported for Dioscorea species (Jiang et al. 2012).

Quantifying the degree of crystallinity is a key application of XRD, and is especially valuable for materials that contain both crystalline and amorphous phases. It is classified as a semi-crystalline polymer, with its crystalline regions mainly attributed to amylose and the amorphous regions of amylopectin. XRD analysis in this study revealed a calculated relative crystallinity of 34.3% for *A. paeoniifolius* starch, a result that closely aligns with previous literature findings (Jiang et al. 2012). Further comparisons with other starches revealed that Yam Starch (YS) and Taro Starch (TS) exhibited crystallinity levels of 32.88% and 44.66%, respectively (Andrade et al. 2017).

XRD-Specific Surface Area and Morphology Index

A. paeoniifolius starch powder is widely utilized across multiple industries, including the food, pharmaceutical, drug delivery, cosmetic, and paper industries. The specific surface area (SSA) of the amorphous starch powder was determined based on the relationship between the particle size and morphology index (MI), as presented in Table 4. The MI is calculated based on the full width at half maximum (FWHM) values obtained from the XRD data and provides a quantitative measure of particle morphology, and consequently, its SSA.

The MI is defined as the ratio between the FWHM value of the peak with the greatest intensity and the FWHM value of a specific reference peak. This provides a quantitative measure of particle morphology, which is outlined by the following Equation 4:

$$M.I = \frac{FWHM_h}{FWHM_h + FWHM_p} \quad \ldots(4)$$

where $FWHM_h$ is the highest FWHM value, and $FWHM_p$ is the FWHM value of a particular peak (Theivasanthi & Alagar 2011). This index aids in correlating particle size and shape, which are crucial factors in understanding the applications of starch across various industries. The experimental MI values for *A. paeoniifolius* starch powder ranged from 0.50 to 0.67, as shown in Table 4. A strong positive correlation was observed between MI and particle

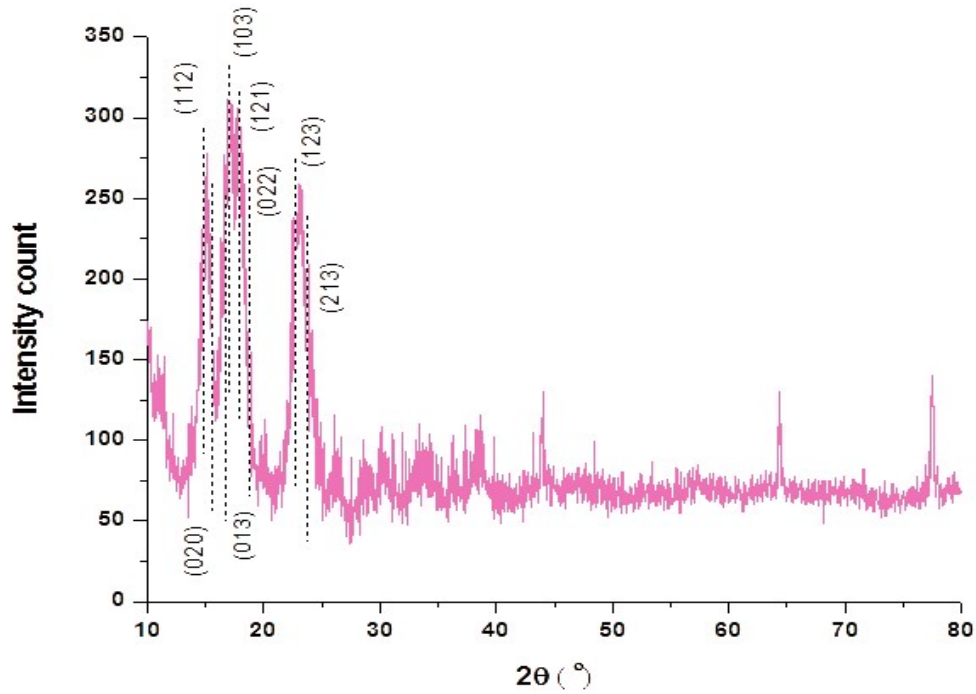

Fig. 5: X-ray diffraction (XRD) pattern of *Amorphophallus paeoniifolius* starch.

Table 4: Morphology index and specific surface area of *A. paeoniifolius* particles.

FWHM (Full Width at Half Maximum) (β) (radians)	Particle Size (D) [nm]	Morphology Index	SSA [$m^2.g^{-1}$]
0.0145	9.9043	0.5808	757.2456
0.0099	14.4470	0.6686	519.138
0.0140	10.3777	0.5897	722.7006
0.0131	11.0908	0.6053	676.2332
0.0129	11.2867	0.6085	664.5002
0.0171	8.5371	0.5399	878.5135
0.0187	8.0646	0.5180	929.9901
0.0201	7.5477	0.5000	993.6761

size; that is, as MI increased, particle size also tended to increase, whereas MI showed a near-perfect negative correlation with SSA. As the MI increased, the SSA decreased. SSA is a fundamental property of materials that provides critical insights into material identification and characterization. SSA denotes the surface area available per unit mass and is particularly significant in applications involving adsorption, heterogeneous catalysis, and surface-related reactions. This parameter is essential for assessing materials for various industrial and scientific applications, as it influences their reactivity, stability, and effectiveness in specific roles. It is calculated using the formula presented in Equation 5.

$$S = \frac{6*10^3}{D_p \rho} \quad \ldots(5)$$

where S represents the specific surface area (SSA), Dp denotes the particle size, and ρ signifies the density of *A. paeoniifolius* starch, which was measured at 0.8 grams per cubic centimeter. This relationship is instrumental in calculating the SSA, as it accounts for both the particle size and material density, thereby providing a comprehensive assessment of the surface area per unit mass.

CONCLUSIONS

This study comprehensively evaluated the physicochemical properties of *A. paeoniifolius* starch, a less-explored tropical tuber, highlighting its potential as a sustainable material for bioplastics and food packaging applications. Characterization using DSC, FTIR, XRD, SEM, and EDX indicated the potential suitability of starch for producing biodegradable films. The results showed that *A. paeoniifolius* starch exhibited stable thermal properties, molecular integrity, and a semi-crystalline structure with a crystallinity index of 34.3%. Proximate composition analysis revealed a high starch content of 78.61%, a moisture content of 11.8%, and low fat content (0.30%), suggesting its viability as a carbohydrate-rich raw material. However, the film-forming ability and mechanical performance were not directly tested in this study. Preliminary findings suggest that this starch could be used in biodegradable packaging applications with further optimization. Future research should focus on optimizing film preparation and processing to enhance the mechanical, barrier, and thermal properties for large-scale applications.

ACKNOWLEDGMENT

The authors are grateful to the Department of Biotechnology, Jaypee Institute of Information Technology, Noida, Uttar Pradesh, India, for providing the necessary facilities to execute this work.

REFERENCES

Abbas, K.A., Khalil, S.K. and Hussin, A.S.M., 2010. Modified starches and their usages in selected food products: A review study. *Journal of Agricultural Science*, 2(2), pp.90. [DOI]

Abdullah, A.H.D., Chalimah, S., Primadona, I. and Hanantyo, M.H.G., 2018. Physical and chemical properties of corn, cassava, and potato starchs. *IOP Conference Series*. *Earth and Environmental Science*, 160, 012003. [DOI]

Abegunde, O.K., 2012. Physicochemical characterization of starches from some Nigerian and Chinese roots and tubers. *African Journal of Food Science*, 6(11). [DOI]

Alonso-Gomez, L., Niño-López, A.M., Romero-Garzón, A.M., Pineda-Gomez, P., del Real-Lopez, A. and Rodriguez-Garcia, M.E., 2016. Physicochemical transformation of cassava starch during fermentation for production of sour starch in Colombia: Transformation of cassava starch during fermentation. *Die Stärke*, 68(11–12), pp.1139–1147. [DOI]

Alozie, Y.E., Iyam, M.A., Lawal, O., Udofia, U. and Ani, I.F., 2009. Utilization of bambara groundnut flour blends in bread production. *Journal of Food Technology*, 7(4), pp.111-114.

Andrabi, S.N., Wani, I.A., Gani, A., Hamdani, A.M. and Masoodi, F.A., 2016. Comparative study of Physicochemical and functional properties of starch extracted from two kidney bean (Phaseolus vulgaris L.) and green gram cultivars (Vigna radiata L.) grown in India. *Starch-Stärke*, 68(5–6), pp.416–426.

Andrade, L.A., Barbosa, N.A. and Pereira, J., 2017. Extraction and properties of starches from the non-traditional vegetables yam and taro. *Polímeros*, 27(2), pp.151–157. [DOI]

Galvão, A.M.M.T., de Oliveira Araújo, A.W., Carneiro, S.V., Zambelli, R.A. and Bastos, M.D.S.R., 2018. Coating development with modified starch and tomato powder for application in frozen dough. *Food Packaging and Shelf Life*, 16, pp.194–203. [DOI]

Aprianita, A., Purwandari, U., Watson, B. and Vasiljevic, T., 2009. Physico-chemical properties of flours and starches from selected commercial tubers available in Australia. *International Food Research Journal*, 16(4), pp.507–520.

Araújo, R.G., Rodríguez-Jasso, R.M., Ruiz, H.A., Govea-Salas, M., Rosas-Flores, W., Aguilar-González, M.A., Pintado, M.E., Lopez-Badillo, C., Luevanos, C. and Aguilar, C.N., 2020. Hydrothermal–microwave processing for starch extraction from Mexican avocado seeds: Operational conditions and characterization. *Processes*, 8(7), 759. [DOI]

Ashaolu, T.J., 2020. Soy bioactive peptides and the gut microbiota modulation. *Applied Microbiology and Biotechnology*, 104(21), pp.9009–9017. [DOI]

Awuchi, C.G., Chukwu, C.N., Iyiola, A.O., Noreen, S., Morya, S., Adeleye, A.O., Twinomuhwezi, H., Leicht, K., Mitaki, N.B. and Okpala, C.O.R., 2022. Bioactive compounds and therapeutics from fish: Revisiting their suitability in functional foods to enhance human wellbeing. *BioMed Research International*, 2022, 3661866. [DOI]

Boahemaa, L.V., Dzandu, B., Amissah, J.G.N., Akonor, P.T. and Saalia, F.K., 2024. Physico-chemical and functional characterization of flour and starch of taro (Colocasia esculenta) for food applications. *Food and Humanity*, 2, 100245. [DOI]

Cone, J.W. and Wolters, M.G.E., 1990. Some properties and degradability of isolated starch granules. *Die Stärke*, 42(8), pp.298–301. [DOI]

Cummings, J.H. and Stephen, A.M., 2007. Carbohydrate terminology and classification. *European Journal of Clinical Nutrition*, 61 Suppl 1, pp.S5-S18. [DOI]

Esquivel-Fajardo, E.A., Martinez-Ascencio, E.U., Oseguera-Toledo, M.E., Londoño-Restrepo, S.M. and Rodriguez-García, M.E., 2022. Influence of physicochemical changes of the avocado starch throughout its pasting profile: Combined extraction. *Carbohydrate Polymers*, 281, 119048. [DOI]

Geirnaert, A., Calatayud, M., Grootaert, C., Laukens, D., Devriese, S., Smagghe, G., De Vos, M., Boon, N. and Van de Wiele, T., 2017. Butyrate-producing bacteria supplemented in vitro to Crohn's disease patient microbiota increased butyrate production and enhanced intestinal epithelial barrier integrity. *Scientific Reports*, 7(1), 11450. [DOI]

Gernat, C., Radosta, S., Damaschun, G. and Schierbaum, F., 1990. Supra molecular structure of legume starches revealed by X-ray scattering. *Die Stärke*, 42(5), pp.175–178. [DOI]

Gupta, R. and Gaur, S., 2024. Investigating the effect of natural fermentation in modifying the physico-functional, structural and thermal characteristics of pearl and finger millet starch. *Journal of the Science of Food and Agriculture*, 104(4), pp.2440–2448. [DOI]

Hamaker, B.R. and Griffin, V.K., 1993. Effect of disulfide bond-containing protein on rice starch gelatinization and pasting. *Cereal Chemistry*, 70(4), pp.377–380.

He, Y., Wang, B., Wen, L., Wang, F., Yu, H., Chen, D., Su, X. and Zhang, C., 2022. Effects of dietary fiber on human health. *Food Science and Human Wellness*, 11(1), pp.1–10. [DOI]

Huang, H., Krishnan, H.B., Pham, Q., Yu, L.L. and Wang, T.T.Y., 2016. Soy and gut microbiota: Interaction and implication for human health. *Journal of Agricultural and Food Chemistry*, 64(46), pp.8695–8709. [DOI]

Ijarotimi, O.S., Fagbemi, T.N. and Osundahunsi, O.F., 2015. Evaluation of nutrient composition, glycaemic index and anti-diabetic potentials of multi-plant based functional foods in rats. *Sky Journal of Food Science*, 4(6), pp.78–90.

Indian Standard (IS), 2022. Infant Food - Milk-Cereal Based Complementary Foods - Specification. IS 1656:2022. Bureau of Indian Standards, Govt. of India.

Indian Standard (IS), 1981. Specification for Ready-to-Protein-Rich Extruded Foods. IS 9487:1981. Bureau of Indian Standards, Govt. of India.

Indian Standard (IS), 2019. Method for Estimation of Total Dietary Fibre in Foodstuffs. IS 11062:2019. Bureau of Indian Standards, Govt. of India.

Indian Standard (IS), 1975. Specification for Bombay Halwa. IS 2650:1975. Bureau of Indian Standards, Govt. of India.

Islam, F., Noman, M., Afzaal, M., Saeed, F., Ahmad, S., Zubair, M.W., Zahra, S.M., Hussain, M., Ateeq, H. and Awuchi, C.G., 2022. Synthesis and food applications of resistant starch-based nanoparticles. *Journal of Nanomaterials*, 2022(1). [DOI]

Jiang, Q., Gao, W., Li, X., Xia, Y., Wang, H., Wu, S., Huang, L., Liu, C. and Xiao, P., 2012. Characterizations of starches isolated from five different Dioscorea L. species. *Food Hydrocolloids*, 29(1), pp.35–41. [DOI]

Jubril, I., Muazu, J. and Mohammed, G.T., 2012. Effects of phosphate modified and pregelatinized sweet potato starches on disintegrant property of paracetamol tablet formulations. *Journal of Applied Pharmaceutical Science*, pp.32–36.

Julianti, E., Rusmarilin, H., Ridwansyah and Yusraini, E., 2018. Effect of isolation methods on physicochemical properties of purple-fleshed sweet potato starch. In: *Proceedings of the International Conference of Science, Technology, Engineering, Environmental and Ramification Researches (ICOSTEERR 2018) - Research in Industry*, 4, pp.37-41.

Kandekar, U.Y., Abhang, T.R., Pujari, R.R. and Khandelwal, K.R., 2021. Exploration of elephant foot yam (Amorphophallus paeoniifolius) starch: An alternative natural disintegrant for pharmaceutical application. *Indian Journal of Pharmaceutical Education*, 55(1s), pp.s209–s219. [DOI]

Kaur, M. and Sandhu, K.S., 2010. Functional, thermal and pasting characteristics of flours from different lentil (Lens culinaris) cultivars. *Journal of Food Science and Technology*, 47(3), pp.273–278. [DOI]

Kibret Akalu, Z. and Haile Geleta, S., 2019. Comparative analysis on the proximate composition of tubers of Colocasia esculenta, L. schott and Dioscorea alata cultivated in Ethiopia. *American Journal of Bioscience and Bioengineering*, 7(6), pp.93. [DOI]

Levitsky, A.P., Egorov, B.V., Lapinskaya, A.P. and Selivanskaya, I.A., 2020. Inadequate fat diet. *Journal of Education, Health and Sport*, 10(7), pp.248–255. [DOI]

Liang, X. and King, J.M., 2003. Pasting and crystalline property differences of commercial and isolated rice starch with added amino acids. *Journal of Food Science*, 68(3), pp.832–838. [DOI]

Lumdubwong, N. and Seib, P.A., 2000. Rice starch isolation by alkaline protease digestion of wet-milled rice flour. *Journal of Cereal Science*, 31(1), pp.63–74. [DOI]

M.S., Chagam Koteswara Rao, Sundaramoorthy, H. and N., H., 2018. Influence of debranching and retrogradation time on behavior changes of Amorphophallus paeoniifolius nanostarch. *International Journal of Biological Macromolecules*, 120(Pt A), pp.230–236. [DOI]

Marichelvam, M.K., Jawaid, M. and Asim, M., 2019. Corn and rice starch-based bio-plastics as alternative packaging materials. *Fibers*, 7(4), 32. [DOI]

Marimuthu, M., Sundaram, U. and Gurumoorthi, P., 2013. X-ray diffraction and starch analysis of nano-sized seed powder of velvet bean (Mucuna pruriens). *Indo American Journal of Pharmaceutical Research*, 3(2).

Meludu, N.T., 2010. Proximate analysis of sweet potato toasted granules. *African Journal of Biomedical Research*, 13(1), pp.89–91.

Bureau of Indian Standards (BIS), 1978. Methods of tests for edible starches and starch products. IS 4706:1978.

Mohammed, A. and Abdullah, A., 2018. Scanning electron microscopy (SEM): A review. In: *Proceedings of the 2018 International Conference on Hydraulics and Pneumatics-HERVEX*, pp.7–9.

Mukherjee, A., Banerjee, A., Sinhababa, A. and Singh, P.P., 2014. The genus Amorphophallus: Cyto-histo-molecular genesis and commercial prospects. *International Journal of Innovative Horticulture*, 3, pp.12–21.

Olkku, J. and Rha, C., 1978. Gelatinisation of starch and wheat flour starch—A review. *Food Chemistry*, 3(4), pp.293–317. [DOI]

Omar, K.A., Salih, B.M., Abdulla, N.Y., Hussin, B.H. and Rassul, S.M., 2016. Evaluation of starch and sugar content of different rice samples and study their physical properties. *Indian Journal of Natural Sciences*, 6(36), pp.11084–11088.

Omodamiro, R.M., Afuape, S.O., Njoku, C.J., Nwankwo, I.I.M., Echendu, T.N.C. and Edward, T.C., 2013. Acceptability and proximate composition of some sweet potato genotypes: Implication of breeding for food security and industrial quality. *International Journal of Biotechnology and Food Science*, 1(5), pp.97–101.

Oyom, W., Zhang, Z., Bi, Y. and Tahergorabi, R., 2022. Application of starch-based coatings incorporated with antimicrobial agents for preservation of fruits and vegetables: A review. *Progress in Organic Coatings*, 166, 106800. [DOI]

Özdamar, E.G. and Ateş, M., 2018. Rethinking sustainability: A research on starch based bioplastic. *Journal of Sustainable Construction Materials and Technologies*, 3, pp.249–260.

Reddy, C.K., Haripriya, S., Noor Mohamed, A. and Suriya, M., 2014. Preparation and characterization of resistant starch III from elephant foot yam (Amorphophallus paeonifolius) starch. *Food Chemistry*, 155, pp.38–44. [DOI]

Rodriguez-Garcia, M.E., Hernandez-Landaverde, M.A., Delgado, J.M., Ramirez-Gutierrez, C.F., Ramirez-Cardona, M., Millan-Malo, B.M. and Londoño-Restrepo, S.M., 2021. Crystalline structures of the main components of starch. *Current Opinion in Food Science*, 37, pp.107–111. [DOI]

Saikia, J.P. and Konwar, B.K., 2012. Physicochemical properties of starch from aroids of North East India. *International Journal of Food Properties*, 15(6), pp.1247–1261. [DOI]

Schoch, T.J., 1968. Preparation and properties of various legume starches. *Cereal Chemistry*, 45, pp.564–573.

Shujun, W., Jinglin, Y. and Wenyuan, G., 2005. Use of X-ray diffractometry (XRD) for identification of Fritillaria according to geographical origin. *American Journal of Biochemistry & Biotechnology*, 1(4), pp.207–211. [DOI]

Shujun, W., Wenyuan, G., Hongyan, L., Haixia, C., Jiugao, Y. and Peigen, X., 2006. Studies on the physicochemical, morphological, thermal and crystalline properties of starches separated from different Dioscorea opposita cultivars. *Food Chemistry*, 99(1), pp.38–44. [DOI]

Singh, A. and Wadhwa, N., 2014. A review on multiple potential of aroid: Amorphophallus paeoniifolius. *International Journal of Pharmaceutical Sciences Review and Research*, 24(1), pp.55–60.

Sondari, D., Falah, F., Suryaningrum, R., Sari, F.P., Septefani, A.A., Restu, W.K. and Sampora, Y., 2019. Biofilm based on modified sago starch: Preparation and characterization. *Reaktor*, 19(3), pp.125–130. [DOI]

Indian Standard, 1973. Method of determination of protein in foods and feeds. IS 7219:1973.

Indian Standard, 1975. Specification for edible groundnut flour (expeller-pressed). IS 4684:1975.

Sukhija, S., Singh, S. and Riar, C.S., 2016. Isolation of starches from different tubers and study of their physicochemical, thermal, rheological and morphological characteristics: Characterization of tuber starches. *Die Stärke*, 68(1–2), pp.160–168. [DOI]

Theivasanthi, T. and Alagar, M., 2011. An insight analysis of nano sized powder of jackfruit seed. *Nano Biomedicine and Engineering*, 3(3). [DOI]

Titov, V.N., 2012. Regulation of insulin fatty acid metabolism, and then glucose in the implementation of the biological function of locomotion. *Clinical Laboratory Diagnosis*, 5, pp.3–12.

Wahyuningtiyas, N.E. and Suryanto, H., 2017. Analysis of biodegradation of bioplastics made of cassava starch. *Journal of Mechanical Engineering Science and Technology*, 1(1), pp.24–31. [DOI]

Witek, K., Wydra, K. and Filip, M., 2022. A high-sugar diet consumption, metabolism and health impacts with a focus on the development of substance use disorder: A narrative review. *Nutrients*, 14(14), 2940. [DOI]

Yusuf, F., Kubo, A.I., Abdulrashid, F.U., Madu, S.J. and Muazu, J., 2022. Studies on the physicochemical properties of coprocessed starch obtained from Ipomoea batatas. *Nigerian Journal of Basic & Applied Sciences*, 30(2). [DOI]

Zhang, S., Fan, X., Lin, L., Zhao, L., Liu, A. and Wei, C., 2017. Properties of starch from root tuber of Stephania epigaea in comparison with potato and maize starches. *International Journal of Food Properties*, 20(8), pp.1740–1750. [DOI]

Zhou, W., Apkarian, R., Wang, Z.L. and Joy, D., 2007. *Scanning Microscopy for Nanotechnology: Techniques and Applications*. Springer, pp.1–40.

Zobel, H.F., 1988. Starch crystal transformations and their industrial importance. *Die Stärke*, 40(1), pp.1–7. [DOI]

Zuo, Y., He, X., Li, P., Li, W. and Wu, Y., 2019. Preparation and characterization of hydrophobically grafted starches by in situ solid phase polymerization. *Polymers*, 11(1), 72. [DOI]